

Automatic Generation of Seamline Network Using Area Voronoi Diagrams With Overlap

Jun Pan, Mi Wang, Deren Li, and Jonathan Li, *Member, IEEE*

Abstract—The mosaicking of orthoimages has been used to cover a large geographic region for various applications ranging from environmental monitoring to disaster management. However, existing mosaicking methods mainly focus on the generation of seamlines between two adjacent orthoimages. In this paper, we present a novel approach based on the use of a seamline network formed by a novel area Voronoi diagrams with overlap and the use of effective mosaic polygons (EMPs) to define the pixels of each orthoimage for the final mosaic. The generated seamline network is global based and is also optimized after refinement. It gives an effective partitioning for the regions of all orthoimages to form EMPs. The partitioning is unique, seamless, and has no redundancy. The algorithm is parallel, and the EMP of each orthoimage only has relation to orthoimages which have overlaps with it. It can ensure the flexibility and efficiency of mosaicking, without an intermediate process and independent of the sequence of the image composite. The experimental results obtained from the mosaicking of 40 color orthoimages demonstrate considerable potential for generating a seamline network automatically and effectively. This is extremely useful when a seamless mosaic is required to cover a large geographic region.

Index Terms—Orthoimage mosaic, remote sensing, seamline network, Voronoi diagrams.

I. INTRODUCTION

MOSAICKING is the process of combining multiple images into a single seamless composite image. It is possible to mosaic unrectified individual frames or flight lines of remotely sensed data [1]. However, it is more common to mosaic multiple images that have already been orthorectified to a standard map projection and datum. Such orthorectified images are also called orthoimages. They normally will overlap a certain amount (e.g., 20%–30%). They integrate the rich information content of images and the geometric properties of maps (ground projection) and can be easily combined with

Manuscript received April 16, 2008; revised September 3, 2008. First published April 21, 2009; current version published May 22, 2009. The work was supported in part by the National Basic Research Program of China (973 Program) under Grant 2006CB701302, in part by National High-tech R&D Program (863 Program) under Grant 2009AA12Z120 and in part by the Outstanding Youth Foundation Plan of Wuhan under Grant 200750731253.

J. Pan, M. Wang, and D. Li are with the State Key Laboratory of Information Engineering in Surveying, Mapping and Remote Sensing, Wuhan University, Wuhan, 430079, China (e-mail: hero_pj@126.com; wangmi@x263.net; drli@whu.edu.cn).

J. Li is with the Department of Geography and Environmental Management, Faculty of Environment, University of Waterloo, Waterloo, ON N2L 3G1, Canada, and also with the State Key Laboratory of Information Engineering in Surveying, Mapping and Remote Sensing, Wuhan University, Wuhan 430079, China (e-mail: junli@uwaterloo.ca).

Color versions of one or more of the figures in this paper are available online at <http://ieeexplore.ieee.org>.

Digital Object Identifier 10.1109/TGRS.2008.2009880

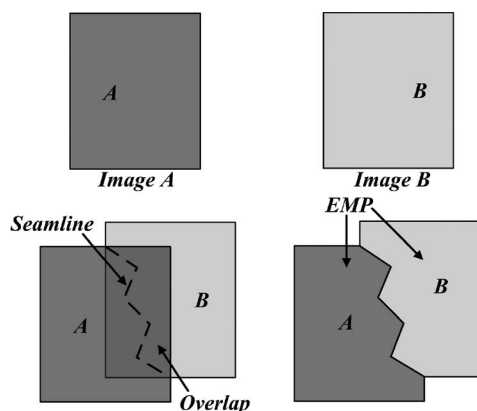


Fig. 1. Illustration of seam-based mosaicking.

additional information from geographic information systems (GISs) to create an orthoimage map. Thus, they have become a popular visualization product and planning instrument [2].

In most instances, if two images are taken from even slightly different angles, shadows or glares will be different on given objects. Then, a nonseam-based mosaic is likely to yield a picture that does not correspond closely to reality [3]. Therefore, the seam-based mosaicking of orthoimages becomes more and more popular. An illustration of the seam-based mosaicking of two orthoimages is shown in Fig. 1. A seamline is defined in the overlap region. Then, in mosaicking, each pixel in the final mosaicking result is represented entirely by only one orthoimage based on which side of the seamline it lies on. Finally, there is the specific objective of making the seam invisible in the final [3]. In the procedure, each region of orthoimages is, in fact, partitioned by seamlines into effective mosaic polygons (EMP). The EMP defines the useful part of each orthoimage, and the mosaic is considered as a composite of these useful parts based on EMPs. When mosaicking more than two orthoimages, each pixel is represented entirely by only one orthoimage based on which EMP of the orthoimage the pixel lies in. To this end, we can eliminate redundancy in mosaicking, particularly for remotely sensed images with a high percentage of overlap. Therefore, it is critical to generate seamlines and form the EMPs based on these generated seamlines in seam-based mosaicking in terms of efficiency.

Studies on seam-based mosaicking have mainly focused on the generation of seamlines between the adjacent orthoimages and did not consider how to connect the individual seamlines to generate EMPs [2]–[7]. Based on the generated seamlines, a frame-to-frame method [8] is used to stitch the orthoimages successively, which recursively combines each new frame to

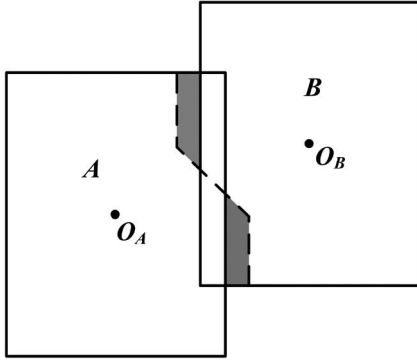


Fig. 2. Seamline generated by the ordinary Voronoi diagrams of frame centers based on the Manhattan distance for two images.

the mosaic formed from previous frames [9]. However, the frame-to-frame method is still a sequential approach and has drawbacks of low efficiency, requirement of intermediate process, and dependence on the composite sequence. Hsu *et al.* [8] presented a local-to-global method adopting the ordinary Voronoi diagrams of frame centers based on the Manhattan distance to generate seamlines and form EMPs in order to reduce these drawbacks. However, the ordinary Voronoi diagrams are based on a point set, whereas the regions of orthoimages constitute an area set. If a point in each orthoimage (e.g., the frame center) is used to constitute a point set, it cannot be ensured that the generated seamlines lie in the overlap of adjacent orthoimages, which may lead to areas not covered by any orthoimage. As shown in Fig. 2, O_A and O_B are the frame centers of images A and B , respectively. The dashed line between images A and B represents the seamline generated by the ordinary Voronoi diagrams of frame centers based on the Manhattan distance. Two parts of the generated seamline are located outside the overlap area of the adjacent images A and B . Using such seamline to mosaicking, the two shaded areas are neither covered by image A nor image B in the final mosaic. Xandri *et al.* [10] presented an approach to connecting individual seamlines to generate EMPs. They defined a seamline by finding a path that minimizes the cost crossing the image in overlap and classifying the seamlines into two catalogues: along- and cross-strip seams. Different from that of Xandri *et al.* [10], our method takes an advantage of geometric information to generate the initial seamline network globally followed by refining the generated seamline network.

The Voronoi diagrams are one of the most fundamental data structures in computational geometry and have been applied widely in many fields for space partitioning. In order to meet all kinds of practical requirements, the ordinary Voronoi diagrams have been extended continuously, and many generalized Voronoi diagrams have been presented. The comprehensive overviews of these models and their applications in a variety of fields can be found in [11]–[14]. Some new extensions of Voronoi diagrams and their applications have been presented in [15]–[19]. The regions of orthoimages compose a set of areas with overlaps. In fact, it is a space partitioning issue for a set of areas with overlaps to generate EMPs for orthoimages. In this paper, a novel area Voronoi diagrams with overlap (AVDO) is presented. Based on AVDO, we propose an automatic approach

to generate a seamline network for producing orthoimage mosaics covering a large geographic area and to refine the initial seamline network based on the pixel values in the overlaps in the following.

II. AVDO

Definition 2.1: Let $A = \{A_1, A_2, \dots, A_n\}$ be a finite set of distinct areas in the 2-D Cartesian space R^2 . In A , the arbitrary area is not belonging to another area, but two arbitrary areas may overlap each other. Let A_i and A_j be the two arbitrary distinct areas in A . Let $A_i \cap A_j = O_j$, $A_i = A'_i \cup O_j$, $A_j = A'_j \cup O_j$, p be an arbitrary point in $A_i \cup A_j$, and $d_a(p, A_i, A_j)$ be the Euclidean distance between point p and area A_i in the restriction of A_j . The $d_a(p, A_i, A_j)$ is defined as the minimum Euclidean distance between point p and an arbitrary point in A'_i , the nonoverlapping part of A_i between A_i and A_j .

If $A_i \cap A_j \neq \phi$, we have

$$d_a(p, A_i, A_j) = \min_{q \in A'_i} d(p, q). \quad (1)$$

Obviously, if $p \in A'_i$, $d_a(p, A_i, A_j) = 0$.

$B(A_i, A_j)$ is defined as the bisector of A_i and A_j , which is represented by

$$B(A_i, A_j) = \{p | d_a(p, A_i, A_j) = d_a(p, A_j, A_i), p \in A_i \cup A_j\}. \quad (2)$$

Obviously, the distances from an arbitrary point on $B(A_i, A_j)$ to areas A_i and A_j are equal.

Then, the region $V(A_i, A_j)$ is defined as the Voronoi polygon associated with A_i in the restriction of A_j by the set of locations in $A_i \cup A_j$ satisfying the condition, $d_a(p, A_i, A_j) \leq d_a(p, A_j, A_i)$, which is represented by

$$V(A_i, A_j) = \{p | d_a(p, A_i, A_j) \leq d_a(p, A_j, A_i), p \in A_i \cup A_j\}. \quad (3)$$

If $A_i \cap A_j = \phi$, then $A_i = A'_i$ and $A_j = A'_j$, $\forall p \in A_i \cup A_j$, $d_a(p, A_i, A_j) = \min_{q \in A'_i} d(p, q)$. Obviously, $\forall p \in A_i$, $d_a(p, A_i, A_j) = 0 < d_a(p, A_j, A_i)$ and $V(A_i, A_j) = A_i$; $\forall p \in A_j$, $d_a(p, A_j, A_i) = 0 < d_a(p, A_i, A_j)$ and $V(A_j, A_i) = A_j$. Namely, the area without overlap to A_i has no effect on the generation of the Voronoi polygon for A_i . Because there is no overlap between the two areas, the bisector $B(A_i, A_j)$ does not exist.

Let p be an arbitrary point in A , $I_n = \{1, 2, \dots, n\}$, and $d_a(p, A_i)$ be the Euclidean distance between point p and area A_i . Then, $d_a(p, A_i)$ is given by

$$d_a(p, A_i) = \max_{j \in I_n, j \neq i} d_a(p, A_i, A_j) \quad (4)$$

and the Voronoi polygon of arbitrary area A_i is represented by

$$\begin{aligned} V(A_i) &= \bigcap_{j \in I_n, j \neq i} V(A_i, A_j) \\ &= \{p | d_a(p, A_i) \leq d_a(p, A_j), j \neq i, j \in I_n, p \in A\}. \end{aligned} \quad (5)$$

Namely, the Voronoi polygon of A_i is only related to areas having overlap with A_i . Then, the Voronoi polygon of the arbitrary

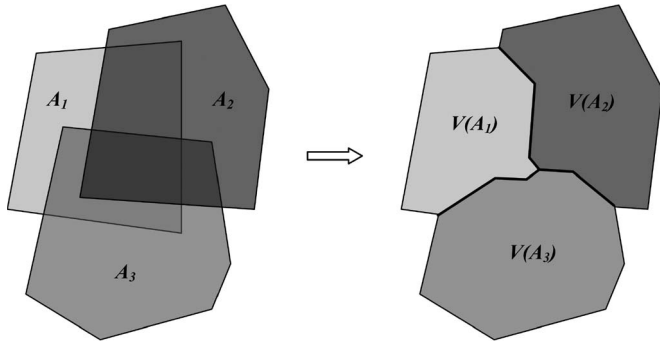


Fig. 3. Voronoi diagrams of $A = \{A_1, A_2, A_3\}$.

area A_i can be simplified further. Let $A_{m1}, A_{m2}, \dots, A_{mm}$ be the m ($0 \leq m < n$) areas which have overlap with A_i , and $m1, m2, \dots, mm \in I_n$. Then, the Voronoi polygon of A_i can be simplified as

$$V(A_i) = \bigcap_{j \in I_m} V(A_i, A_{mj}). \quad (6)$$

Then, the Voronoi polygon set of all areas in $A = \{A_1, A_2, \dots, A_n\}$ form the AVDO of A

$$V = \{V(A_1), V(A_2), V(A_3), \dots, V(A_n)\}. \quad (7)$$

The Voronoi edge is the common edge of two adjacent Voronoi polygons ($V(A_i) \cap V(A_j) \neq \phi$)

$$\begin{aligned} V_E(A_i, A_j) &= V(A_i) \cap V(A_j) \\ &= \{p | d_a(p, A_i) = d_a(p, A_j) \leq d_a(p, A_k), \\ &\quad k \neq i \neq j, k \in I_n, p \in A\}. \end{aligned} \quad (8)$$

The Voronoi vertex is the intersection point of at least three Voronoi polygons ($V(A_i) \cap V(A_j) \cap V(A_k) \neq \phi$)

$$\begin{aligned} V_V(A_i, A_j, A_k) &= V(A_i) \cap V(A_j) \cap V(A_k) \\ &= V_E(A_i, A_j) \cap V_E(A_i, A_k) \\ &\quad \cap V_E(A_j, A_k) \\ &= \{p | d_a(p, A_i) = d_a(p, A_j) \\ &\quad = d_a(p, A_k) \leq d_a(p, A_l), \\ &\quad l \neq i \neq j \neq k, l \in I_n, p \in A\}. \end{aligned} \quad (9)$$

Fig. 3 shows the Voronoi diagrams of the area set $A = \{A_1, A_2, A_3\}$. The major properties of the AVDO are summarized as follows.

- 1) The region for partitioning is the union of all areas, and it allows overlap between adjacent areas.
- 2) The partitioning to the area set is unique, seamless, and has no redundancy.
- 3) The Voronoi edge lies in the overlapping part between adjacent areas, and the Voronoi vertex lies in the multi-overlapping part among areas.

III. METHODS

Based on the AVDO, an automatic algorithm for the generation of a seamline network is developed. The algorithm applies

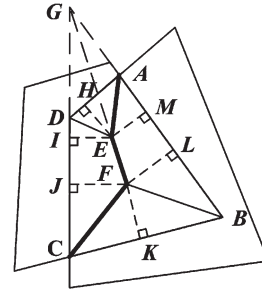


Fig. 4. Generation of bisectors between two adjacent images.

the generated seamline network to partition regions of orthoimages into the EMPs. It has the following three advantages:

- 1) effective partitioning for the regions of all orthoimages, which makes it clear which pixels in each image contribute to the final mosaic;
- 2) high processing efficiency as the final mosaic can be directly obtained, independent of the composite sequence;
- 3) no intermediate process involved.

When the AVDO is used to generate the seamline network, the EMP of each orthoimage is precisely corresponded to the generated Voronoi polygon, and each seamline is precisely the common edge of the two adjacent Voronoi polygons. According to the definition of the AVDO, the Voronoi polygons are generated based on the bisector between the adjacent orthoimages with overlap. Therefore, the bisectors should be calculated first, followed by the construction of the Voronoi polygons. Finally, the common edges of the adjacent Voronoi polygons are obtained. Each common edge is a seamline, and all of the seamlines form a seamline network.

A. Generation of Bisectors

Most of the remote sensing images acquired by airborne and satelliteborne sensors are captured along strips, and mosaicking these images to cover a large geographic region is one of the routine tasks at the mapping agencies or companies. Without loss of generality, the region of each orthoimage can be approximately denoted as a quadrangle (rectangle is the special case), and the overlap of the adjacent orthoimages is still a quadrangle. In other words, we can assume that the overlap of any two adjacent orthoimages is a quadrangle when dealing with remotely sensed images.

The steps for generating the bisectors between the adjacent orthoimages with overlap are shown in Fig. 4 and described as follows.

- Step 1) Calculate the overlap of adjacent orthoimages. Without loss of generality, let $ABCD$ be the quadrangle of the overlap, and A and C be the intersection points of the regions of adjacent orthoimages.
- Step 2) Calculate the angular bisectors of the four internal angles of $ABCD$, and let them be AE , DE , DF , and CF , respectively. Let E be the closest intersection point to A between the angular bisector of $\square A$ and other three angular bisectors, and let F be the closest intersection point to C between the angular

bisector of $\square C$ and other three angular bisectors. Then, the polyline $AEFC$ is just the bisector of the two adjacent images.

B. Generation of Voronoi Polygons

The bisectors are only the cutting lines between the adjacent orthoimages with overlap. The Voronoi polygons can be generated based on the bisectors. It is suggested that all of the bisectors should be used to generate the Voronoi polygon for each orthoimage. The procedure is described by the following pseudocodes:

```

For each orthoimage I DO
{
  For each orthoimage J DO
  {
    If image I and image J have overlap,
    {
      Step 1. Calculate the bisector;
      Step 2. Use the bisector to clip the region of
orthoimage I;
      Step 3. Use the clipping result to update the
region of orthoimage I;
    }
  }
}

```

In this way, the region of the orthoimage will be clipped continuously to form a Voronoi polygon of the orthoimage. Then, the regions of all orthoimages will be partitioned into Voronoi polygons.

In Step 2), the clipping operation of using the bisector to clip the region of the orthoimage is referred to as the polygon clipping algorithm [20], [21]. The main idea is as follows. For each orthoimage, when using a bisector related to it to clip its region, the overlap of the two adjacent orthoimages is regarded as the reference to determine whether an intersection point is an entry or exit point. The entry and exit points are in pairs. From an entry point, follow the chain of bisector vertices until the next exit point is reached. Then, jump to the clipped polygon and follow the chain of polygon vertices until the next entry point is reached. Repeat the aforementioned tracing process until the initial starting point is reached, and then, the clipping operation is finished. The chain of traced vertices is the result of clipping. Some definitions used in the clipping operation are as follows.

Definition 3.1: Inner area and outer area of the polygon.

The direction of edges of the polygon is the order that the vertices of the polygon are inputted, clockwise or counterclockwise. If the direction of edges of the polygon is clockwise, then along the edges, the right area is the inner area of the polygon, and the left area is the outer area of the polygon; on the contrary, if the direction of edges of the polygon is counterclockwise, then along the edges, the left area is the inner area, and the right area is the outer area. For the polygon with holes, the edges of inner holes should have the opposite direction compared with the edges of outer boundary.

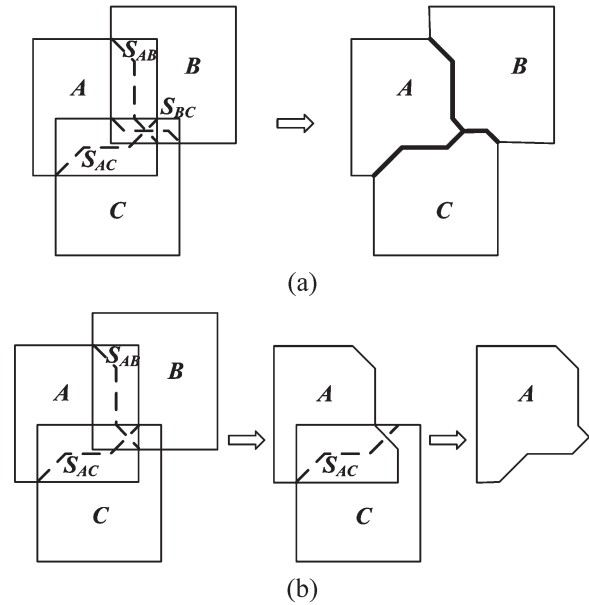


Fig. 5. Generation of Voronoi polygons.

Definition 3.2: Entry point and exit point.

Let I be an intersection point of polygons S and C . Along the direction of edges, if polygon S enters polygon C from outer to inner at point I , then point I is an entry point with reference to polygon C . On the contrary, if polygon S exits polygon C from inner to outer at point I , then point I is an exit point with reference to polygon C .

Definition 3.3: Determination of the entry and exit points.

Assume that edge $S_i S_{i+1}$, an edge of polygon S , has intersection points with polygon C . When S_i is out of polygon C , along the edge direction of polygon C , the first intersection point of edge $S_i S_{i+1}$ and polygon C , which is point I , must be the entry point with reference to polygon C ; when S_i is in polygon C , point I must be the exit point with reference to polygon C . Because the entry and exit points are in pairs (aside from the case that two polygons intersect at vertex or they have common edges), it is only necessary to determine whether the first intersection point is an entry or exit point, and then, other intersection points can be determined in turn by the characteristic that the entry and exit points are in pairs.

The generation of a Voronoi polygon is shown in Fig. 5. The arrangement of regions for orthoimages A , B , and C is shown in the left of Fig. 5(a), and the dashed lines S_{AB} , S_{AC} , and S_{BC} are bisectors. The bisector S_{AB} is the bisector between the regions of orthoimages A and B . The bisector S_{AC} is the bisector between the regions of orthoimages A and C . The bisector S_{BC} is the bisector between the regions of orthoimages B and C . The Voronoi polygons for the three orthoimages are shown in the right of Fig. 5(a). The Voronoi polygon generation for orthoimage A is shown in Fig. 5(b). The bisectors S_{AB} and S_{AC} are necessary for the Voronoi polygon generation of orthoimage A . The region of orthoimage A is first clipped by S_{AB} , and then, the former clipped result is further clipped by S_{AC} . The final result is precisely the Voronoi polygon of orthoimage A . In the same way, the Voronoi polygons of orthoimages B and C can also be generated.

C. Generation of Seamline Network

The seamline network is the network formed by connecting individual seamlines. On the one hand, it plays the role of partitioning the region of each orthoimage; on the other hand, it is the fundamental of the feathering and color transition in mosaicking. A common edge of two adjacent Voronoi polygons is precisely the seamline between the two orthoimages, and it is a polyline. After generating Voronoi polygons, all the individual seamlines will be obtained by calculating all the common edges between Voronoi polygons, and the seamline network will be formed by connecting individual seamlines. Moreover, it is still necessary to construct the topological relation between seamlines and Voronoi polygons to benefit the mosaicking, e.g., to determine the adjacent Voronoi polygons to each seamline, the corresponding orthoimage to each Voronoi polygon, and the corresponding overlap to each seamline.

The seamline network generated in this way is only a partitioning to the regions of all orthoimages in geometry. With reference to individual seamlines, they are blind to scene content and are not optimal. Objects not included in the digital terrain model or wrongly modeled objects appear at different locations in the overlap of adjacent orthoimages, i.e., geometric differences may exist. Moreover, radiometric or color differences between neighboring orthoimages may also exist. These differences cause additional problems in mosaicking. Therefore, further refinement of the seamline network is needed.

D. Refinement of Seamline Network

The refinement of the seamline network aims at making seamlines avoid passing through high difference areas. It includes the refinement of Voronoi vertices, i.e., junction nodes of individual seamlines, and individual seamlines. The refinement of Voronoi vertices is carried out in the corresponding multi-overlapping areas. Assume that the Voronoi vertex lies in the n -overlapping area A , i.e., there are n images (F_1, F_2, \dots, F_n) overlapping with each other. The cost for pixel (x, y) is defined as

$$D(x, y) = \max_{i,j=1,\dots,n,i \neq j} D_{ij}(x, y). \quad (10)$$

In the formula, $D_{ij}(x, y)$ is the cost of pixel (x, y) for images i and j , which is defined as [10]

$$D_{ij}(x, y) = \max_{k=1,\dots,n} |F_i^k(x, y) - F_j^k(x, y)|. \quad (11)$$

In which, k is the band number of image. Then, the refined Voronoi vertex is

$$V(x, y) = \min_{(x,y) \in A} D(x, y). \quad (12)$$

The refinement of individual seamlines is carried out in the overlapping area, and in fact, it is a path-seam problem from the starting point to the ending point. We use the bottleneck model [3] to solve this problem.

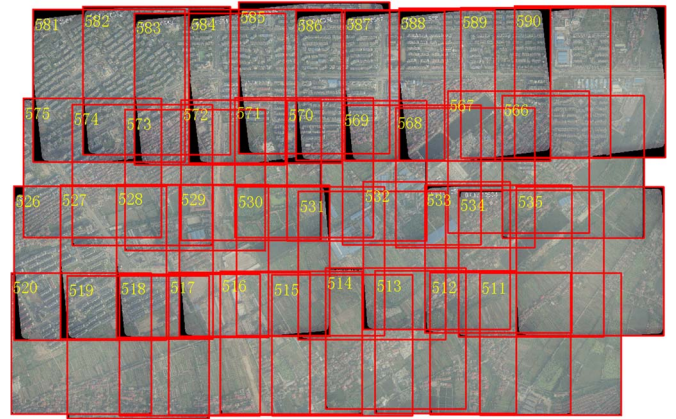


Fig. 6. Arrangement of the regions of orthoimages.



Fig. 7. Initial seamline network formed by AVDO.



Fig. 8. Refined seamline network.

The cost of pixel (x, y) is defined as (11). A path seam PS is a simple path from the starting point to the ending point, and the refinement of any individual seamline is to find a path with a cost as small as possible. Let image i be the left image and image j be the right image; then, the cost of any PS is defined as

$$f(PS) = \max_{(x,y) \in PS} D_{ij}(x, y), \quad (13)$$

The refined individual seamline is a path seam which could minimize $f(PS)$.

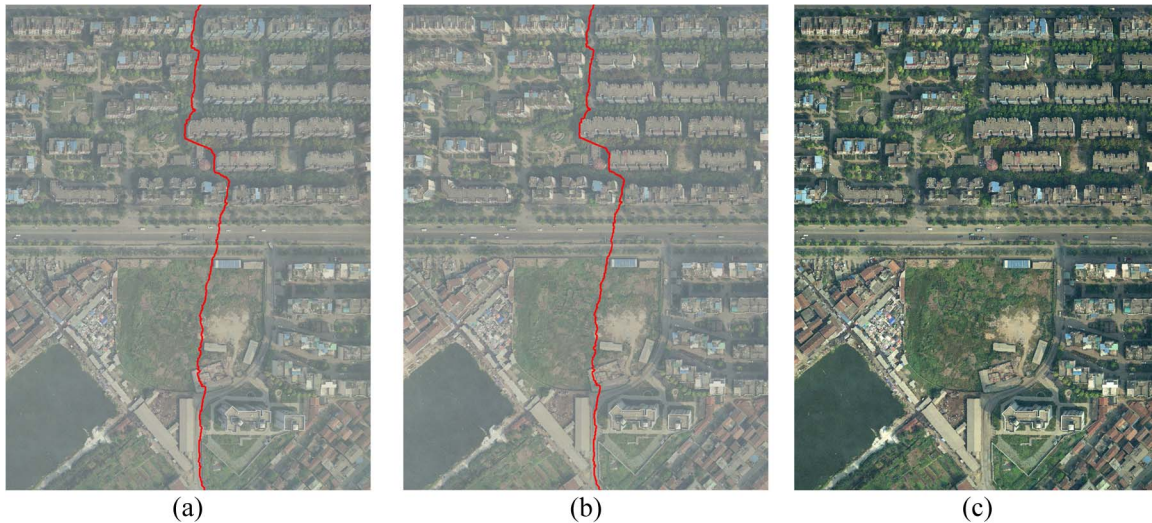


Fig. 9. Details of refined seamline. (a) Left image overlapping refined seamline, (b) right image overlapping refined seamline, and (c) mosaicking result.

Usually, the algorithm can provide paths that are not simple, i.e., some pixels can have more than two neighbors. Moreover, the path seam is searched in raster format, and when transforming into vector format, too many points will aggravate the computation burden of the mosaicking processing. Therefore, we use the Douglas–Peucker algorithm to finally simplify the refined individual seamlines. After the refinement, the corresponding Voronoi polygons, i.e., EMPs, should also be updated.

IV. EXPERIMENTAL RESULTS

Our algorithm was applied into the mosaicking. The mosaicking process used in this study includes the following steps: 1) to do the color balancing to minimize the radiometric differences between different orthoimages; 2) to generate the initial seamline network using AVDO; 3) to refine the seamline network using the pixel values in the overlaps; 4) to do the image composite; and 5) to do the feathering along the seamlines to achieve a seamless mosaic.

The generation of seamline networks is one key step in mosaicking. The generated initial seamline network based on AVDO is the coarse seamlines, and then, it is refined using the pixel values of images. Different from that of Afek and Brand [9], in our method, the seamline networks are globally generated, and the regions of orthoimages are partitioned into EMPs. We also compared our EMP-based method with the frame-to-frame method in the mosaicking experiments.

The data sets used in this study are the 40 orthoimages generated from four strips of color aerial images covering a study area in the City of Wuhan, Hubei, China. These images were captured in 2006 with an approximate endlap of 64% and a sidelap of 45%. Each strip consists of ten images. The resolution of the orthoimage is 0.2 m, and the image size is approximately 3800 by 3800 pixels. A desktop computer with an Intel Pentium 4 CPU at 2.4 GHz and an internal memory with a capacity of 1.5 GB, and a hard disk with a capacity of 320 GB, 8-MB cache, and 7200 r/min was used for the data processing.

The arrangement of the regions of orthoimages is shown in Fig. 6, and orthoimages were placed according to their

geocoding information. Each orthoimage was denoted by a rectangle and labeled by its filename at the upper left corner. The generated initial seamline network based on AVDO is shown in Fig. 7. The regions of orthoimages were partitioned into EMPs, i.e., the generated Voronoi polygons. The common edges between Voronoi polygons are individual seamlines, and all individual seamlines connecting with each other form the initial seamline network. The refined seamline network overlapping the final mosaic according to the geocoding information is shown in Fig. 8. Furthermore, Fig. 9 shows the detail of a refined seamline. Fig. 9(a) shows the left image overlapping the refined seamline, Fig. 9(b) shows the right image overlapping the refined seamline, and Fig. 9(c) shows the mosaicking result. Obviously, after refinement, individual seamlines and Voronoi vertices are all optimized. The regions of all orthoimages are partitioned effectively, and there are no overlaps or missing parts between the EMPs. To this end, each pixel in the mosaic belongs uniquely to one orthoimage. The final mosaicking result validates the proposed approach.

In the experiment, we also counted the computation time when testing our algorithm. It took 109 ms to generate the initial seamline network based on AVDO and 412 266 ms to refine the seamline network. A comparison of our EMP-based method with the frame-to-frame method is given in Table I. Our EMP-based method uses the AVDO to generate the initial seamline network followed by the refinement of the generated seamline network. The generated seamline network is global, and the generating algorithm is parallel. By doing so, we can construct the final mosaic directly, without an intermediate process and independent of the sequence of image composite. In addition, it is easy to avoid defective areas, for example, the heavy cloudy areas in remotely sensed images, just by editing the seamlines to eliminate these cloudy areas from the EMPs. However, when using the frame-to-frame method, one has to generate the mosaic first and patch the cloudy areas subsequently. It cannot finish the processing at one time.

Our experiments demonstrate that it took the frame-to-frame method 595 140 ms and our EMP-based method 373 812 ms to complete the image composite of 40 orthoimages. The image

TABLE I
COMPARISON OF FRAME-TO-FRAME METHOD WITH OUR EMP-BASED METHOD

Method	Items	Global	Parallel	Independence of the sequence of image composite	Without intermediate results	Easy to avoid defective areas	Image composite time for the test data set (ms)
EMP-based		Yes	Yes	Yes	Yes	Yes	373812
Frame-to-frame		No	No	No	No	No	595140

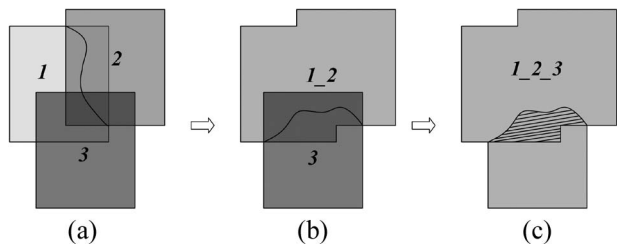


Fig. 10. Illustration of the frame-to-frame method.

composite by each method was optimized by the scan-line filling algorithm to improve the efficiency. The comparison shows that our method reduces the computation time by 37.2% and therefore has a higher efficiency. As shown in Fig. 10, there are pixels which are read and written twice or more times when using the frame-to-frame method. For example, when using the frame-to-frame method to make a mosaic of three images, named images 1, 2, and 3, the mosaicking is done by following the image sequence from 1, 2, and 3. In other words, the seamline between images 1 and 2 is generated first [see Fig. 10(a)] followed by the mosaicking of the images 1 and 2 to form a new image 1_2 [see Fig. 10(b)]. The seamline between images 1_2 and 3 is then generated [Fig. 10(b)] followed by the mosaicking of images 1_2 and 3 to form the final mosaic. To this end, the pixels in the shaded area in Fig. 10(c) will be read and written twice. However, in our EMP-based method, each pixel will only be read and written once. This is why our method can reduce the image composite time significantly. This is extremely useful when generating a mosaic to cover a large geographic region. For the orthoimages with a large percentage of overlap, our method will have much more advantages than the frame-to-frame method in terms of computation efficiency.

V. CONCLUSION

In this paper, we have presented a new idea on the automatic generation of a seamline network through a two-step operation: globally generating the initial seamline network followed by refining the generated seamline network. Our experimental results demonstrate that the refined seamline network provides considerable potential to improve the efficiency of seamless mosaicking. The partitioning is unique, seamless, and has no redundancy, and the region of each orthoimage is partitioned into an EMP. The use of EMPs ensures flexibility and efficiency of mosaicking. Compared with the frame-to-frame method, the EMP-based method has several advantages, including the following: 1) the final mosaic can be directly constructed based on EMPs without any intermediate process involved, therefore having a higher mosaicking efficiency; 2) the generation of the EMP for each orthoimage is only related to the adjacent orthoimages with overlap, therefore, it can be done simulta-

neously; and 3) the final mosaic is independent of the image composite sequence. Also, it is easy for the EMP-based method to avoid defective areas, for example, the heavy cloudy areas. The experimental results also indicate that our method can generate the initial seamline network very fast and effectively form EMPs for all orthoimages. However, it took more time to refine the generated seamline network. To this end, we suggest that one should not do the refinement for the applications where the processing speed is paid much more attention on than the processing effect, for example, a quick preview of the mosaicking results.

Nevertheless, optimization algorithms for the generation of an initial seamline network needs to be investigated in order to meet more complex mosaic requirements, such as arbitrary shapes for regions and arbitrary arrangement for orthoimages. In addition, the refinement of the initial seamline network should be improved in terms of both the computational efficiency and the optimal seamline searching. These issues will be addressed in our future work.

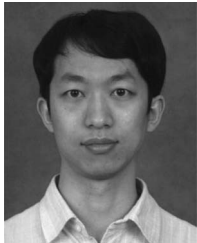
ACKNOWLEDGMENT

The images used in this study were provided by Wuda Geoinformatics Company, Ltd., Wuhan, China. The authors would like to thank the anonymous reviewers for their valuable comments in giving this paper a better presentation.

REFERENCES

- [1] J. R. Jensen, *Introductory Digital Image Processing: A Remote Sensing Perspective*, 3rd ed. Upper Saddle River, NJ: Prentice-Hall, 2005.
- [2] M. Kerschner, "Seamline detection in colour orthoimage mosaicking by use of twin snakes," *ISPRS J. Photogramm. Remote Sens.*, vol. 56, no. 1, pp. 53–64, Jun. 2001.
- [3] E. Fernández, R. Garfinkel, and R. Arbiol, "Mosaicking of aerial photographic maps via seams defined by bottleneck shortest paths," *Oper. Res.*, vol. 46, no. 3, pp. 293–304, May/Jun. 1998.
- [4] D. L. Milgram, "Computer methods for creating photomosaics," *IEEE Trans. Comput.*, vol. C-24, no. 11, pp. 1113–1119, Nov. 1975.
- [5] Y. Shiren, L. Li, and G. Peng, "Two-dimensional seam-point searching in digital image matching," *Photogramm. Eng. Remote Sens.*, vol. 55, pp. 49–53, 1989.
- [6] W. Schickler and A. Thorpe, "Operational procedure for automatic true orthophoto generation," *Int. Arch. Photogramm. Remote Sens.*, vol. 32, no. 4, pp. 527–532, 1998.
- [7] E. Fernández and R. Martí, "GRASP for seam drawing in mosaicking of aerial photographic maps," *J. Heuristics*, vol. 5, no. 2, pp. 181–197, Jul. 1999.
- [8] S. Hsu, H. S. Sawhney, and R. Kumar, "Automated mosaics via topology inference," *IEEE Comput. Graph. Appl.*, vol. 22, no. 2, pp. 44–54, Mar./Apr. 2002.
- [9] Y. Afek and A. Brand, "Mosaicking of orthorectified aerial image," *Photogramm. Eng. Remote Sens.*, vol. 64, no. 2, pp. 115–125, 1998.
- [10] R. Xandri, F. Pérez, V. Palà, and R. Arbiol, "Automatic generation of seamless mosaics over extensive areas from high resolution imagery," in *Proc. World Multi-Conf. Systemics, Cybern. Informat.*, Orlando, FL, 2005.
- [11] F. Aurenhammer, "Voronoi diagrams—A survey of a fundamental data structure," *ACM Comput. Surv.*, vol. 23, no. 3, pp. 345–405, 1991.

- [12] F. Aurenhammer and R. Klein, "Voronoi diagrams," in *Handbook of Computational Geometry*, J. Sack and J. Urrutia, Eds. Amsterdam, The Netherlands: Elsevier, 2000, pp. 201–290.
- [13] A. Okabe, B. Boots, K. Sugihara, and S. N. Chiu, *Spatial Tessellations. Concepts and Applications of Voronoi Diagrams*. Chichester, U.K.: Wiley, 2000.
- [14] A. Okabe, B. Boots, and K. Sugihara, "Nearest neighborhood operations with generalized Voronoi diagrams: A review," *Int. J. Geogr. Inf. Syst.*, vol. 8, no. 1, pp. 43–71, 1994.
- [15] J. Chen, R. L. Zhao, and Z. L. Li, "Voronoi-based k-order neighbour relations for spatial analysis," *ISPRS J. Photogramm. Remote Sens.*, vol. 59, no. 1/2, pp. 60–72, Aug. 2004.
- [16] P. Alliez, É. C. de Verdière, O. Devillers, and M. Isenburg, "Centroidal Voronoi diagrams for isotropic surface remeshing," *Graph. Models*, vol. 67, no. 3, pp. 204–231, May 2005.
- [17] T. Asano, N. Katoh, H. Tamaki, and T. Tokuyama, "Angular Voronoi diagram with applications," in *Proc. ISVD*, Banff, AB, Canada, Jul. 2–5, 2006, pp. 32–39.
- [18] R. Reitsma, S. Trubin, and E. Mortensen, "Weight-proportional space partitioning using adaptive Voronoi diagrams," *Geoinformatica*, vol. 11, no. 3, pp. 383–405, Sep. 2007.
- [19] R. Wein, J. P. van den Berg, and D. Halperin, "The visibility-Voronoi complex and its applications," *Comput. Geom.*, vol. 36, no. 1, pp. 66–87, Jan. 2007.
- [20] K. Weiler and P. Atherton, "Hidden surface removal using polygon area sorting," in *Proc. SIGGRAPH*, 1977, pp. 214–222.
- [21] Y. K. Liu, Y. Gao, and Y. G. Huang, "An efficient algorithm for polygon clipping," *J. Softw.*, vol. 14, no. 4, pp. 845–856, Apr. 2003.



Jun Pan received the B.Eng. degree in geographic information science and the M.Sc. and Ph.D. degrees in photogrammetry and remote sensing from Wuhan University, Wuhan, China, in 2002, 2005, and 2008, respectively.

Since 2008, he has been an Assistant with the State Key Laboratory of Information Engineering in Surveying, Mapping, and Remote Sensing (LIESMARS), Wuhan University. His research focuses on digital image processing, including restoration, image dodging, and quality evaluation,

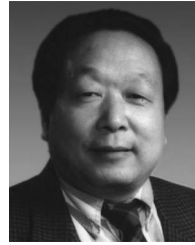
seamless image mosaicking and radiometric normalization, and true orthoimage generation.



Mi Wang received the B.Eng., M.Sc., and Ph.D. degrees in photogrammetry and remote sensing from Wuhan University, Wuhan, China, in 1997, 1999, and 2001, respectively.

Since 2008, he has been a Professor with the State Key Laboratory of Information Engineering in Surveying, Mapping and Remote Sensing, Wuhan University. His research interests include measurable seamless stereo orthoimage databases, geographic information systems (GISs), and the integration of global navigation satellite systems, remote sensing,

and GISs.



Deren Li received the Ph.D. degree in photogrammetry from the University of Stuttgart, Stuttgart, Germany, in 1986.

He is currently a Professor and the Chair of the Academic Committee of the State Key Laboratory for Information Engineering in Surveying, Mapping and Remote Sensing, Wuhan University, Wuhan, China. He was the President of the former Wuhan Technical University of Surveying and Mapping (1996–2000). He has published eight books and more than 400 papers. His current research interests include photogrammetry and remote sensing, global navigation satellite systems, and geographic information systems (GISs), and their innovation integrations and applications in China.

Dr. Li was elected Academician of the Chinese Academy of Sciences, in 1991, the Chinese Academy of Engineering, and the Euro-Asia Academy of Sciences, in 1995. He was the President of the Chinese Society of Geodesy, Photogrammetry and Cartography, and of the International Society for Photogrammetry and Remote Sensing Commissions III and VI. He is the Vice President of the China Society of Image and Graphics, a Chief Scientist of the Optics Valley of China, and the Cochair of the Committee on Earth Observation and Satellites and the Integrated Global Observing Strategy Partnership. He was the founding President of the Asia GIS Association (2003–2006). In the 1980s, his research findings on a posterior variance estimation-based iteration weighted method for bundle location was recognized internationally and named the "Deren Li Method." His research on the separability theory of model errors "scientifically solved a hundred-year baffling problem in geodetic science" and earned him the 1988 Best Paper Award of the German Society for Photogrammetry and Remote Sensing and the Hansa Luftbild Award. He has been the recipient of more than ten national and provincial level awards and prizes, such as the Sci-tech Progress Award, National Excellent Textbook Award, the Excellent Educational Achievement Awards, etc.



Jonathan Li (M'00) received the Ph.D. degree in geomatics engineering from the University of Cape Town, South Africa, in 2000.

In 2000, he was with the Department of Geography, University of Regina, SK, Canada, as an Assistant Professor. From 2001 to 2006, he was an Assistant and Associate Professor and the Director of the Virtual Environment Laboratory, Department of Civil Engineering, Ryerson University, Toronto, ON, Canada. He is currently an Associate Professor with the Department of Geography and Environmental

Management, Faculty of Environment, University of Waterloo, Waterloo, ON, and a Guest Professor at the State Key Laboratory for Information Engineering in Surveying, Mapping and Remote Sensing, Wuhan University, Wuhan, China. His current research interests include cartographic object extraction from image and range data, object-oriented classification, mobile mapping, and integrated geomatics solutions for disaster management. He has been an Associate Editor of the journal *Geomatica* since 2007. He has coedited four books and coauthored more than 100 research articles.

Dr. Li serves the Canadian National Committee for the International Society for Photogrammetry and Remote Sensing (ISPRS) (2002–2012). He is the Chair of the ISPRS Working Group VI/I on Land-based Mobile Mapping Systems (2008–2012) and the Vice Chair of the International Cartographic Association Commission on Mapping from Satellite Imagery (2008–2011). He was a recipient of the 2008 Environmental Systems Research Institute Award for best scientific paper in geographic information systems and the 2007 MDA Award for best technical paper in photogrammetry and surveying.